Astron. Astrophys. 337, 887–896 (1998)

ASTRONOMY AND ASTROPHYSICS

LRC-circuit analog of current-carrying magnetic loop: diagnostics of electric parameters

V.V. Zaitsev[1], **A.V. Stepanov**[2], **S. Urpo**[3], **and S. Pohjolainen**[3]

[1] Applied Physics Institute, N. Novgorod, Russia
[2] Pulkovo observatory, St. Petersburg, Russia
[3] Metsähovi Radio Research Station, Helsinki University of Technology, Espoo, Finland

Received 6 October 1997 / Accepted 4 March 1998

Abstract. The equation for an equivalent LRC-circuit of current-carrying magnetic loop is obtained. It is suggested that the electric current, driven by the converging flows in the photosphere, flows trough the coronal part of a loop from one footpoint to another, and closes deep in the photosphere where plasma beta $\beta \approx 1$. In a self-consistent approach both the capacitance and the resistance of a LRC-circuit depend on the electric current along the loop. This opens new possibilities for the diagnostics of electric currents in coronal loops, by using data on high-quality modulation of microwave emission during flares. Spectral analysis of the Metsähovi millimeter wave solar data for 16 solar flares have revealed modulation periods 0.7–17 s which give currents $I \approx 6\times10^{10}$–1.4×10^{12} A. For two of the events we could compare the total energy of the electric current stored in the magnetic loop with the energy released in the flare. Only 5% of the total energy of the electric circuit was released in both flares, suggesting a very low influence of these flares on the magnetic loop structure. In the studied events there was a tendency to decrease the energy release with the increase of the current. This tendency is interpreted in terms of plasma beta, which is getting smaller as the current grows. Therefore the plasma instabilities responsible for the flare process manifestate themselves weakly with the increase of the current.

Key words: Sun: corona – Sun: flares – Sun: radio radiation

1. Introduction

The last twenty-five years of solar observations in optical, radio, and X-ray bands have revealed the geometry and main characteristics of solar flares. The flare energy release occurs in a coronal magnetic loop or loop system with typical length of a few times 10^9 cm, the cross-sectional area $\approx 10^{17}$ cm^2, the plasma temperature $T \approx 10^6$–10^7 K, and the number density $n \approx 10^{10}$–10^{11} cm^{-3} (Bray et al. 1991). Severny (1965) has evaluated the vertical currents at the photospheric level using magnetograph measurements, indicating currents $I \approx 10^{11}$–10^{12} A in an active region. With this current the resistance $R \approx 10^{-4}$–10^{-3} Ω is required to explain the flare energy release rate $W = RI^2 = 10^{19}$–10^{21} W. Nevertheless, there are no adequate methods now for the diagnostics of electric currents in the coronal magnetic loops.

However, there are a lot of indications on long-term quasiperiodical modulations in flare emission during the flares. Zarro et al. (1987) have concluded that there were quasiperiodic (12–20 s) modulations in the soft X-ray emission in the three flares observed by SMM. Such $\leq$ 20% modulations were interpreted as local variations of the plasma temperature ($\Delta T \approx 5\times10^6$ K), caused by a repeated energy injection to a coronal loop, and due to the periodical processes of the magnetic field reconnection. The solar event of 7 August 1972, observed by OSO-7 in 2–8 Å and 8–16 Å bands, revealed over 700 cycles of extremely regular 1.6 s oscillations which remained remarkably stable in phase and period, throughout the entire flare (Thomas et al., 1987). Such an effect was explained as the periodic kink mode instability within the magnetic arch. Wülser & Kämpfer (1987) have observed long enduring oscillations of H_α flare emission, with time scales of 7–10 s. Kaufmann et al. (1977) have reported on the 10%-modulation at 7 GHz in the flare burst on 28 March 1976, with the period 4.7 s. The modulation was persistent throughout the entire event, e.g., more than 80 min. The VLA and Trieste observations of type I and type IV radio bursts indicated 12 s pulsations during 20 min (Zlobec et al. 1992). Short-duration quasi-periodic ($\approx$ 10–20 s) light fluctuations beginning after the onset of an intense flare on the Hyades star II Tau and lasting for about 13 min, were reported by Rodono (1974). Andrews (1990) has found quasiperiodic variations in the U-band on AD Leo with periods of the order of 10–40 s, following optical flares for up to 15 min.

Hence in both solar and stellar flares the long-term quasiperiodic variations of the optical, radio and X-ray emission exist. Periodic modulation of solar and stellar flare emission is explained usually in terms of Alfvénic and fast magnetosonic oscillations of coronal magnetic loops (Zaitsev & Stepanov 1982, 1989, Stepanov et al. 1992, Mullan et al. 1992) or as the result of periodical motions of a filament (Zaitsev & Stepanov 1988, Houdebine et al. 1991, Doyle et al. 1990). However, the quality (Q)-factor of MHD-oscillations as well as filament oscillations is not large (Q $\leq$ 10) under coronal conditions. It is

Send offprint requests to: Silja.Pohjolainen@hut.fi

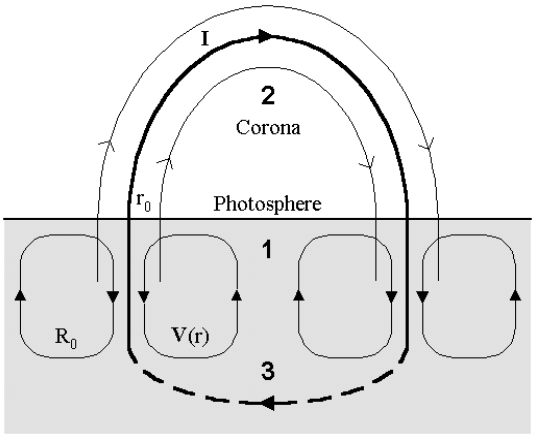

Fig. 1. An electric circuit analog of current-carrying loop. The loop legs locate at the nodes of several supergranulation cells. In region 1, located in the photosphere, electron-atom collision frequency is less compared to the electron gyrofrequency whereas ion-atom collision frequency prevails over the ion gyrofrequency. Both the electric current and the magnetic field grow here, caused by the converging flows of photospheric plasma. Region 2 is the coronal part of a loop. Here $\beta \ll 1$ and the electric current flows along the magnetic field lines. We suppose that deep in the photosphere (region 3) where $\beta \geq 1$ the current flowing through the coronal part of a loop closes between legs

not clear either how one can get high-Q oscillations driven by kink mode instability or magnetic field line reconnection process. Thus there are difficulties in explaining the high quality ($Q \geq 100$) oscillations described above. On the other side, the circuit model for a flare offered by Alfvén & Carlqvist (1967) gives us the possibility to use an equivalent LRC-circuit analog in order to resolve the high-Q problem.

Phenomenological electric circuit approach has been applied to the different problems of solar and stellar physics including flares (e.g., Alfvén & Carlqvist 1967, Spicer 1976, Kan et al. 1983, Melrose & McClymont 1987, Melrose 1991 1995, Zaitsev & Stepanov 1992), filaments (e.g., Kuperus & Raadu 1974, Van Tend & Kuperus 1978, Martens 1987), loop transients (Anzer 1978), heating of the flux tubes (Ionson 1982), as well as the electrodynamics of hot stars (Conti & Underhill 1988), and disk-accreting magnetic neutron star (Miller et al. 1994). Ionson (1982) has considered the electrodynamic coupling between $\beta < 1$ coronal loop plasma and the underlying region with $\beta \geq 1$, where $\beta = 8\pi nkT/B^2$. In this model the main potential magnetic field $\mathbf{B}_\mathrm{o}$ of a loop is generated by a primary dynamo. The resonant coupling of noise e.m.f. driven by the photospheric convection with loop plasma, using LRC-circuit analog, was investigated. Therefore the energy is transferred from convective photospheric noise into the loop plasma, by the Joule dissipation of noise electric currents excited in a loop circuit.

This article addresses the problem of electrodynamics of current-carrying magnetic loop in terms of LRC-circuit. In this case the magnetic field $\mathbf{B}$ of a loop is essentially nonpotential, and is determined by the electric currents flowing throughout the loop but not a primary dynamo that is external to the loop's local mechanical driver as Ionson (1982) had suggested. The reason for the appearance of a current-currying loop can be connected with the photospheric convection (Henoux & Somov 1987). The loop footpoints are located usually at the border of a few supergranules where convective motions produce thin magnetic flux tubes with cross-sectional scales of 100–1000 km and the magnetic field $B \approx 1000$ G. An independent evidence in favour of strong electric currents in a coronal loop is the optical and X-ray data suggesting that the cross-sections of coronal loops vary only 10-20% along the entire length of a loop (Klimchuk et al. 1992).

We show that the main peculiarities of LRC-analog of current-carrying magnetic loops are as follows:

(i) Effective resistance and capacitance of an equivalent LRC-circuit depend on both the mean current value and the screw rate of the magnetic field. There were no evidence on such dependence in previous articles dealing with the calculations of resistance and capacitance of a current-carrying magnetic loop (Spicer 1976).
(ii) The main factor which determines the loop resistance is the loop footpoit area, where effective Joule current dissipation due to ion-atom collisions in partially-ionized plasma, is realized.

As an application of our model we consider here the examples of the diagnostics of the electric currents in coronal loops, using the high-Q oscillations in the Metsähovi mm-wave flare data.

2. Model

To search the properties of an equivalent LRC-circuit of a current-carrying magnetic loop we consider a coronal loop with footpoits imbedded into the photosphere and formed by the converging flow of photospheric plasma. Such a situation can arise, for instance, when the loop footpoints are located in the nodes of several supergranulation cells. An electric circuit analog of such a loop consists of three main domains (Fig. 1).

In region 1, located in the photosphere, the magnetic field and therefore the electric current are generated. In this region the following inequalities are satisfied:

$$\omega_\mathrm{e}/\nu_\mathrm{ea} \gg 1,\ \omega_\mathrm{i}/\nu_\mathrm{ia} \ll 1,\ \omega_\mathrm{e}\omega_\mathrm{i}/\nu_\mathrm{ea}\nu_\mathrm{ia} \gg 1$$

where ω_e and ω_i are the electron and ion gyrofrequencies, ν_ea and ν_ia are 'effective' frequencies for electron-atom and ion-atom collisions, respectively, related with collision frequencies (index o) by

$$\nu_{kl} = (m_l/(m_k + m_l))\nu^o_{kl}$$

Such conditions are thought to excite the radial electric field E_r due to the charge imbalance, which together with the initial magnetic field B_z generates the Hall current j_φ in the azimuthal direction and which, in turn, leads to the increase of B_z (Sen & White 1972). The magnetic field grows up to the value when the field enhancement caused by the converging flow is compensated by the magnetic field diffusion due to the plasma

conductivity. As a result a steady-state flux tube is formed with the magnetic field determined by the total energy input of the convective flux during the time of tube formation (of the order R_0/V_0, where R_0 is the supergranular scale and V_0 is the horizontal velocity of a convective flux). The radius of the flux tube depends on the magnetic field diffusion rate which is due to the conductivity.

Region 2 presents the coronal part of the magnetic loop. Plasma has here $\beta \ll 1$, and the magnetic field is force-free, e.g., the electric currents are parallel to the magnetic field lines.

Region 3 is located probably in the photosphere between the loop footpoints. This is the region of the current closure in an equivalent electric circuit. The photospheric current distribution derived from the magnetograph measurements (see, e.g., Hagyard 1989, Leka et al. 1993) favours an interpretation in terms of an un-neutralized coronal current pattern (Melrose 1991). These data suggest that the magnetic flux tubes carry a current that flows through the coronal part of a loop from one footpoint to the other with no evidence for a return current through the corona. This current must be close along a return path below the photosphere where the magnetic field is not necessarily force-free, and cross-field current can flow along a path of minimum electric resistance, rather that along the magnetic field lines (Hudson 1987, Melrose 1991). There appears to be no theory for how such an un-neutralized current closes below the photosphere.

However, as a first approximation we can assume that the region in the photosphere where this current closes, corresponds to the condition $B^2/8\pi \approx nkT$. The last condition is satisfied by a tube with a magnetic field $B = 1000$ G, and temperature $T = 6\times10^3$ K if the number density $n = 5\times10^{16}$ cm^{-3}, which corresponds to the level $\tau_{5000} = 1$.

3. Basic equations

We start from the equations of three-fluid plasma magnetohydrodynamics for electrons, ions, and neutral atoms. Let us introduce the bulk plasma velocity $\mathbf{V}$ in the laboratory reference frame

$$\mathbf{V} = \frac{\sum_k n_k m_k \mathbf{v}_k}{\sum_k n_k m_k}$$

where k = e, i, a, and $\mathbf{v}_k$ are the velocities of the species in the laboratory reference system. Denote the velocities of the species in the reference frame connected with bulk plasma (diffusion velocities) as $\mathbf{V}_k$. When the diffusion velocities, as well as their derivatives, are small compared with the velocity and acceleration of the bulk plasma (this allows us to consider $d\mathbf{V}_k/dt \approx d\mathbf{V}/\mathrm{dt}$), and the dependence of the friction force due to collisions vs. velocity is linear, the equation of motion for k-th component can be written as

$$\rho_k \frac{d\mathbf{V}_k}{dt} = \rho_k \mathbf{g} - \nabla p_k + n_k q_k \left(\mathbf{E}^* + \frac{1}{c}\mathbf{V}_k \times \mathbf{B}\right) - \sum_l \theta_{kl}(\mathbf{V}_k - \mathbf{V}_l) \quad (1)$$

Here $\mathbf{E}^* = \mathbf{E} + \mathbf{V}\times\mathbf{B}/c$ is the electric field in the reference frame moving with the bulk plasma, $\rho_k = n_k\, m_k$, $q_k = e, -e, 0$ for k = i, e, a, and θ_{kl} is the momentum losses of the k-type particles, due to collisions with particles of l-types. After summing all three equations (1) for each k = e, i, a, and taking the relations

$$\sum_k \rho_k \mathbf{V}_k = 0, \quad \sum_k n_k q_k = 0$$
$$\sum_k n_k q_k \mathbf{V}_k = \mathbf{j}, \quad \sum_{kl} \theta_{kl}(\mathbf{V}_k - \mathbf{V}_l) = 0$$

into account one can get the equation of motion for the bulk plasma

$$\rho \frac{d\mathbf{V}}{dt} = \rho\,\mathbf{g} - \nabla p + \frac{1}{c}\mathbf{j}\times\mathbf{B} \quad (2)$$

where ρ = $n_\mathrm{a} m_\mathrm{a}$ + $n_\mathrm{e} m_\mathrm{e}$ + $n_\mathrm{i} m_\mathrm{i}$ is the density of partially ionized plasma and $\nabla p = \nabla p_\mathrm{a} + \nabla p_\mathrm{i} + \nabla p_\mathrm{e}$.

Excluding from Eq. (1) velocities $\mathbf{V}_k$, after neglecting the terms as small as $(m_\mathrm{e}/m_\mathrm{i})^{1/2}$ in comparison with the units, one can obtain the generalized Ohm's law

$$\mathbf{E}^* = \frac{\mathbf{j}}{\sigma} + \frac{\mathbf{j}\times\mathbf{B}}{enc} - \frac{\nabla p_\mathrm{e}}{en} + \frac{F}{cnm_\mathrm{i}\nu_\mathrm{ia}}\left[(n_\mathrm{a} m_\mathrm{a}\mathbf{g} - \nabla p_\mathrm{a})\times\mathbf{B}\right] - \frac{F^2}{cnm_\mathrm{i}\nu_\mathrm{ia}}\rho\frac{d\mathbf{V}}{dt}\times\mathbf{B} \quad (3)$$

Here $\sigma = ne^2/(m_\mathrm{e}(\nu_\mathrm{ei}+\nu_\mathrm{ea}))$ is conductivity, and $F = \rho_\mathrm{a}/\rho$ is the relative density of neutrals. Eqs. (2) and (3) together with the Maxwell equations and the mass conservation law

$$\frac{\partial\rho}{\partial t} + \mathrm{div}\,(\rho\mathbf{V}) = 0 \quad (4)$$

describe self-consistently the behavior of the plasma and the electromagnetic fields.

4. Current-carrying magnetic flux tubes in the photosphere

The formation of intensive axially symmetric flux tubes with $\mathbf{B}(0, B_\varphi, B_z)$, $\mathbf{j}(0, j_\varphi, j_z)$ in the steady-state situation in the case of axially symmetric $\mathbf{V}(V_r, 0, V_z)$, converging, $V_r < 0$, flux of partially ionized photospheric plasma, supposing the tubes to be vertical inside the convective zone, was considered by Zaitsev (1996, 1997), and Zaitsev & Khodachenko (1997).

Supposing $|\mathbf{V}| \ll V_\mathrm{A}$, C_s, V_g, where V_A, C_s, and V_g are Alfvén, sound and free-fall velocities, respectively we obtain from Eqs. (2) and (3) the following expressions for the magnetic field components of a steady-state flux tube (Zaitsev 1996):

$$\frac{\partial B_z}{\partial r} = \frac{4\pi\sigma V_r}{c^2}\frac{B_z}{1+\alpha\left(B_z^2+B_\varphi^2\right)}$$
$$\frac{1}{r}\frac{\partial\left(rB_\varphi\right)}{\partial r} = \frac{4\pi\sigma V_r}{c^2}\frac{B_\varphi}{1+\alpha\left(B_z^2+B_\varphi^2\right)} \quad (5)$$

where

$$\alpha = \frac{\sigma F}{c^2 n m_i \nu_{ia}}$$

Let us suppose the following approximations for the plasma convection velocity field near a steady-state magnetic flux tube:

$$V_r(r) = V_o r/r_o, \quad V_z(r) = V_{zo} = \text{const}, \quad \text{for } r < r_o$$
$$V_r(r) = V_o r_o/r, \qquad V_z(r) = 0 \qquad \text{for } r > r_o$$

where r_o is the radius of a magnetic flux tube.

For such a model of the convective flow in the photosphere, where $\alpha B^2 \gg 1$, the solution for Eq. (5) can be expressed as (Zaitsev & Khodachenko 1997):

$$B_z^2(r) - B_z^2(0) = \frac{4\pi\sigma V_o r_o}{c^2\alpha}\left(\tilde{r}^2 - b^2 \ln\left|\frac{b^2+\tilde{r}^2}{b^2}\right|\right), \quad \text{for } r \le r_o \tag{6}$$

$$B_\varphi^2(r) = b^2 r_o^2 \frac{B_z^2(r)}{r^2}, \quad \text{for } r \le r_o, \text{and} r > r_o \tag{7}$$

where $b^2 = B_\varphi^2(r_o)/B_z^2(r_o)$, and $\tilde{r} = r/r_o$.

It follows from Eq. (6) that for $V_o < 0$ magnetic field $B_z(r)$ has a maximum on the axis of the tube and decreases with increasing $\tilde{r}$. Assuming that at the tube boundary the magnetic field value $B_z(r_o)$ appears to be much less than $B_z(0)$, we can estimate from Eq. (6) the radius of flux tube (Zaitsev & Khodachenko 1997):

$$r_o = \frac{B_z^2(0)\,F}{4\pi n m_{\rm i}\nu_{\rm ia}|V_o|\left(1 - b^2\ln\left|\frac{1+b^2}{b^2}\right|\right)} \tag{8}$$

In particular, if on the tube boundary $B_\varphi(r_o) = B_z(r_o) \ll B_z(0)$, then for the height $h = 500$ km upon the level $\tau_{5000} = 1$, where $n_{\rm e} \approx 10^{11}$cm^{-3}, $n_{\rm a} \approx 10^{15}$ cm^{-3}, and $T \approx 10^4$K, and the magnetic field on the axis of the flux tube $B_z(0) = 2 \times 10^3$ G, we obtain from Eq. (8) the tube radius $r_o \approx 10^{12}/|V_o|$. This yields for the convection velocity $V_o = 100$ m/s the radius of the magnetic flux tube $r_o = 10^8$ cm.

Keeping in mind that on the boundary of the tube, in the region $r > r_o$, the magnetic field becomes rather small and consequently the photospheric parameters, $\alpha B^2 \ll 1$ and Eq. (5), give the spatial behavior of the magnetic field:

$$B_z(r) = B_z(r_0)\tilde{r}^{-R_{\rm M}}, r > r_o \tag{9}$$

where

$$R_{\rm M} = \frac{4\pi\sigma|V_o|r_o}{c^2}$$

is the magnetic Reynolds number. Thus, we have very rapid power-law decrease of the magnetic field vs. distance for $r > r_o$, because $R_{\rm M} \approx 10^4$ in the photosphere.

Taking Eq. (7) into account we obtain the total longitudinal current I_z in the magnetic flux tube driven by the photospheric convection (Zaitsev 1997):

$$|I_z| = \left|\int_0^\infty 2\pi j_z r dr\right| = \frac{bcr_0}{2}B_z(0) = \frac{B_\varphi(r_o)}{B_z(r_o)}\frac{cr_o}{2}B_z(0)$$

Using Eq. (8) we have

$$|I_z| = \frac{c\,F\,B_z^3(0)\,(\frac{B_\varphi(r_o)}{B_z(r_o)})}{8\pi n m_{\rm i}\nu_{\rm ia}\,|V_o|\,(1 - b^2\ln\left|\frac{1+b^2}{b^2}\right|)} \tag{10}$$

Under the physical conditions of the upper photosphere in height h = 500 km upon the level $\tau_{5000} = 1$, for the plasma flow velocity $|V_o| = 100$ m/s, and the magnetic field $B_z(0) = 2 \times 10^3$ G, Eq. (10) yields for $B_\varphi(r_o) = B_z(r_o)$ the longitudinal current value $I_z = 3 \times 10^{11}$ A.

Thus, thin magnetic flux tubes with strong magnetic field and longitudinal currents of about 10^{11}–10^{12} A can be generated in the photosphere–convection zone. We assume that these currents flow from one footpoint to another through the coronal part of a loop, and close deep down in the photosphere forming an electric circuit.

5. LRC-circuit analog

In the self-consistent model of LRC-circuit both capacitance C and resistance R depend on electric current flowing along the magnetic loop, because the loop structure depends on the current. To find $C(I_z)$ and $R(I_z)$ let us consider the plasma velocity perturbations as well as the perturbations of the electric and magnetic fields driven by small oscillations in the current-carrying magnetic loop. We restrict our approach to Alfvénic-type fluctuations when both pressure and density of the plasma remain constant. For slender flux tubes we introduce a local cylindrical reference frame r_o, φ_o, z_o, in which z_o-axis in each point of the loop is parallel to the loop axis. We introduce also the following designations:

$$B(r,t) = B_{\varphi o}(r) + b(r,t)\,,$$
$$B_z(r,t) = B_{zo}(r) + b_z(r,t)\,, \tag{11}$$
$$V_r(r,t) = V_{ro}(r) + v_r(r,t)$$

where $|B_{\varphi o}| \gg |b_\varphi|, |B_{zo}| \gg |b_z|, |V_{ro}| \gg |v_r|$, and the values of $B_{\varphi o}(r), B_{zo}(r)$, and $V_{ro}(r)$ satisfy Eqs. (5) describing the structure of a steady-state loop. The linearized equations describing region 1 (photosphere-convection zone where the loop footpoints are located) are expressed as

$$\rho\frac{\partial v_r}{\partial t} = \frac{1}{c}\left(j_{\varphi o}b_z + j_{\tilde{\varphi}}B_{zo} - j_{zo}b_\varphi - j_{\tilde{z}}B_{\varphi o}\right) \tag{12}$$

$$E_z + \frac{1}{c}v_r B_{\varphi o} + \frac{1}{c}V_{ro}b_\varphi = \frac{j_{\tilde{z}}}{\sigma} - \frac{F^2\rho}{cnm_{\rm i}\nu_{\rm ia}}\frac{\partial v_r}{\partial t}B_{\varphi o} \tag{13}$$

where

$$j_{\varphi o} = -\frac{c}{4\pi}\frac{\partial B_{zo}}{\partial r}, \quad j_{zo} = \frac{c}{4\pi}\frac{1}{r}\frac{\partial(rB_{\varphi o})}{\partial r},$$
$$j_{\tilde{\varphi}} = -\frac{c}{4\pi}\frac{\partial b_z}{\partial r}, \quad j_{\tilde{z}} = \frac{c}{4\pi}\frac{1}{r}\frac{\partial(rb_\varphi)}{\partial r} \tag{14}$$

here

$$|j_{\varphi o}| \gg |j_{\tilde{\varphi}}|\,, \quad |j_{zo}| \gg |j_{\tilde{z}}|$$

We assume that the eigenfrequencies of an equivalent LRC-circuit for the coronal loop are small compared with the inverse Alfvén transit time in the scale of the order of the loop thickness. In this case the circuit eigenmodes can be considered as adiabatic for the perturbations of the loop magnetic field. It means

that for eigenmodes the magnetic field can be expressed as in the case of a steady-state situation:

$$B_z(r,t) = \frac{r}{br_o} B_\varphi(r,t) \tag{15}$$

Substituting Eq. (11) into Eq. (15) and taking Eqs. (14) into account, we obtain the following relations between the components of the magnetic field and currents:

$$\begin{aligned} B_{zo} &= \frac{r}{br_o} B_{\varphi o}, \quad b_z = \frac{r}{br_o} b_\varphi, \\ j_{\varphi o} &= -\frac{r}{br_o} j_{zo}, \quad j_{\tilde{\varphi}} = -\frac{r}{br_o} j_{\tilde{z}} \end{aligned} \tag{16}$$

Using Eqs. (16) we can write the following expression for the velocity:

$$\rho \frac{\partial v_r}{\partial t} = -\frac{1}{c}\left(1 + \frac{r^2}{b^2 r_o^2}\right)\left(j_{zo} b_\varphi + j_{\tilde{z}} B_{\varphi o}\right) \tag{17}$$

Excluding the velocity from Eq. (13) and by using Eq. (17) we get:

$$\begin{aligned} \frac{\partial E_z}{\partial t} \;=\; & \frac{1}{\sigma}\frac{\partial j_{\tilde{z}}}{\partial t} \\ & + \frac{F^2 B_{\varphi o}}{c^2 n m_{\rm i} \nu_{\rm ia}}\left(1 + \frac{r^2}{b^2 r_o^2}\right)\left(j_{zo}\frac{\partial b_\varphi}{\partial t} + B_{\varphi o}\frac{\partial j_{\tilde{z}}}{\partial t}\right) \\ & + \frac{B_{\varphi o}}{c^2 \rho}\left(1 + \frac{r^2}{b^2 r_o^2}\right)\left(j_{zo} b_\varphi + j_{\tilde{z}} B_{\varphi o}\right) \\ & - \frac{1}{c} V_{ro} \frac{\partial b_\varphi}{\partial t} \end{aligned} \tag{18}$$

We introduce also the average values for the current as well as the magnetic and electric fields:

$$\bar{j}_{zo} = \frac{I_z}{\pi r_o^2}, \quad \bar{j}_{\tilde{z}} = \frac{I_{\tilde{z}}}{\pi r_o^2},$$

$$\bar{B}_{\varphi o} = \frac{I_z}{c r_o}, \quad \bar{b}_\varphi = \frac{I_{\tilde{z}}}{c r_o}, \tag{19}$$

$$\bar{E}_z \;=\; \frac{2}{r_o^2}\int E_z(r) r dr$$

where I_z and $I_{\tilde{z}}$ are the constant and deviated z-components of the electric current in the magnetic flux tube. The integration of Eq. (18) over the cross-section of the loop results in the equation for the loop part in the dynamo region (region 1):

$$\begin{aligned} \frac{\partial \bar{E}_z}{\partial t} \;=\; & \left[\frac{1}{\pi r_o^2 \sigma_1} + \xi \frac{2F^2 I_z^2}{c^4 n m_{\rm i} \nu_{\rm ia} \pi r_o^4}\left(1 + \frac{B_z^2(r_o)}{B_\varphi^2(r_o)}\right)\right]\frac{\partial I_{\tilde{z}}}{\partial t} \\ & + \xi \frac{2 I_z^2}{c^4 \rho_1 \pi r_o^4}\left(1 + \frac{B_z^2(r_o)}{B_\varphi^2(r_o)}\right) I_{\tilde{z}} \end{aligned} \tag{20}$$

where

$$\xi = \frac{\int_o^{r_o}\left(1 + \frac{r^2}{b^2}\right) B_{\varphi o}\left(j_{zo} b_\varphi + j_{\tilde{z}} B_{\varphi o}\right) 2\pi r dr}{\pi r_o^2 \left(1 + \frac{1}{b^2}\right) \bar{B}_{\varphi o}\left(\bar{j}_{zo}\bar{b}_\varphi + \bar{j}_{\tilde{z}}\bar{B}_{\varphi o}\right)}$$

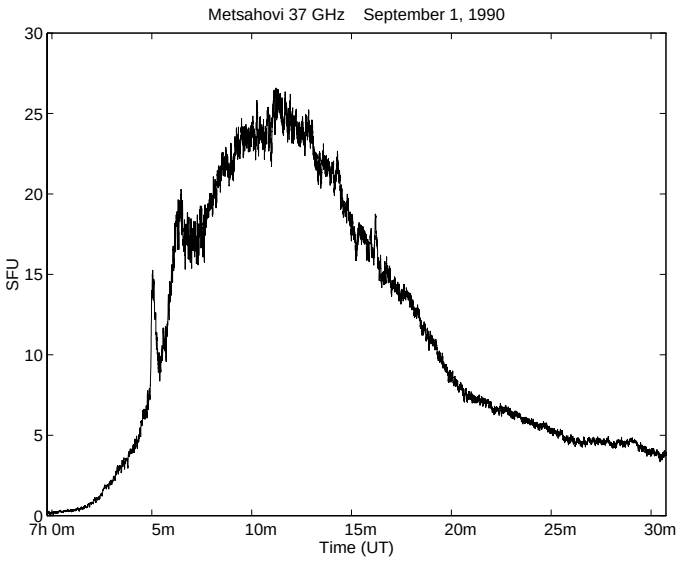

Fig. 2. Solar radio burst observed at Metsähovi Radio Research Station on September 1, 1990

and σ_1 and ρ_1 are the conductivity and the plasma density in the region 1.

Consider now the coronal part of a loop (region 2). We will assume that the currents and magnetic fields in region 2 vary in space according to Eqs. (16). This is due to the fact that Eqs. (5), which result in Eq. (15) for adiabatic magnetic field perturbations ($\omega < V_{\rm A}/r_o$), are true for the coronal part of a loopwhere $\alpha = 0$ (fully ionized plasma). It should be taken into account that the small diffusion plasma flow runs through the loop surface ($V_{ro} \neq 0$) in region 2, because both the plasma density and temperature inside and outside the loop are different. An additional argument in favour of the similarity of the space structure of magnetic fields in photospheric and coronal parts of a loop has been given by the observations of an almost constant loop cross-section along the entire loop length (Klimchuk et al. 1992).

Keeping in mind these arguments we obtain the following equation for the coronal part of the electric circuit (region 2):

$$\frac{\partial \bar{E}_z}{\partial t} = \frac{1}{\pi r_o^2 \sigma_2}\frac{\partial I_{\tilde{z}}}{\partial t} + \xi \frac{2 I_z^2}{c^4 \rho_2 \pi r_o^4}\left(1 + \frac{B_z^2(r_o)}{B_\varphi^2(r_o)}\right) I_{\tilde{z}} \tag{21}$$

where σ_2 and ρ_2 are the conductivity and the plasma density in the region 2.

Deep in the photosphere where the electric current closure between the loop footpoints take place (region 3), we use the formula

$$\frac{\partial \bar{E}_z}{\partial t} = \frac{1}{\sigma_3 S_3}\frac{\partial I_{\tilde{z}}}{\partial t} \tag{22}$$

Here σ_3 and S_3 are the plasma conductivity and the cross-sectional area of the current channel in the region 3.

To describe the global electrodynamics of the current-carrying loop we must integrate $\partial \bar{E}_z/\partial t$ over the entire circuit keeping in mind Eqs. (20), (21), and (22), and the expression

$$\oint \frac{\partial \bar{E}_z}{\partial t} dz = -\frac{L}{c^2}\frac{\partial^2 I_{\tilde{z}}}{\partial t^2}$$

Table 1. Mm-wave bursts with high-Q oscillations and circuit parameters

Date	mm-wave burst time (UT)	Burst max flux (s.f.u.)	Pulse period (s)	Current ($\times 10^{11}$ A)	Circuit energy ($LI^2/2c^2 \times 10^{31}$ erg)	Thermal energy of flare ($\times 10^{29}$ erg)
22 June 1989	14:47–14:59	<150	5.2	2.0	1.0	1–4.5
19 May 1990	13:15–13:40	10	0.7	14.2	50.0	
1 Sept 1990	7:06–7:30	27	1.3	7.7	15.0	
28 Aug 1990	9:00–10:00	100	0.9	11.0	25.4	
28 Aug 1990	10:15–15:00	60	0.9	11.0	25.4	
24 Mar 1991	14:11–14:17	<700	10.0	1.0	0.25	
7 May 1991	10:36–11.00	18	8.3	1.2	0.36	1.3–1.8
11 May 1991	13:22–13:40	<600	6.7	1.5	0.56	
15 Feb 1992	9:35–9:50	3.5	4.8	2.1	1.1	
16 Feb 1992	12:36–13:20	∼2000	5.0	2.0	1.0	
7 July 1992	12:20–12:40	35	7.7	1.3	0.42	
8 July 1992	9:48–!0:10	∼2500	3.3	3.0	2.3	
8 July 1992	10:15–11:00	15	16.7	0.6	0.08	
13 July 1992	8:00–8:16	10	2.0	5.0	6.2	
10 June 1993	6:05–6:35	100	4.0	2.5	1.6	
27 June 1993	11:22–12:00	40	3.5	2.8	2.0	

where L is the circuit inductance. This results in the global electrodynamics equation:

$$\frac{1}{c^2}L\frac{\partial^2 I_{\tilde{z}}}{\partial t^2} + R(I_z)\frac{\partial I_{\tilde{z}}}{\partial t} + \frac{1}{C(I_z)}I_{\tilde{z}} = 0 \tag{23}$$

where $R = R_1 + R_2 + R_3$, and

$$R_1 = \frac{l_1}{\pi r_o^2 \sigma_1} + \xi\frac{2I_z^2 l_1 F^2}{c^4 n m_{\rm i}\nu_{\rm ia}\pi r_o^4}\left(1 + \frac{B_z^2(r_o)}{B_\varphi^2(r_o)}\right) \tag{24}$$

$$R_2 = \frac{l_2}{\pi r_o^2 \sigma_2}\ , \quad R_3 = \frac{l_3}{S_3\sigma_3}\ , \tag{25}$$

$$\frac{1}{C} = \xi\frac{2I_z^2}{c^4\pi r_o^4}\left(1 + \frac{B_z^2(r_o)}{B_\varphi^2(r_o)}\right)\left(\frac{l_1}{\rho_1} + \frac{l_2}{\rho_2}\right) \tag{26}$$

and l_1, l_2, and l_3 are the lengths of the circuits' parts in the dynamo-region, corona, and the region of the current closure, respectively. Eq. (23) suggests that deviated part of the electric current is small compared the current mean value. It opens a possibility for the interpretation of quasi-periodic low amplitude modulation of mcw-emission in terms of eigen oscillations of an equivalent LRC-circuit. Therewith the oscillation period depends on the current mean value.

Some peculiarities should be noted in Eq. (23). First, the steady-state e.m.f. acting in the photospheric dynamo-region is included in Eq. (23) by a self-consistent way via Eqs. (5). This e.m.f. generates the steady-state component of the electric current I_z, persisting in Eq. (23) as a parameter which determines the main characteristics of the equivalent LRC-circuit. Both the circuit resistance R and capacitance C depend on the total current I_z because this current determines the self- consistent magnetic field inside the tube and, as a result, the effective conductivity and the Alfvén velocity. Secondly, the resistance R and capacitance C of the circuit with the given electric current I_z depend on the magnetic field twisting in a loop, $B_z^2(r_o)/B_\varphi^2(r_o)$. Thirdly, it is easy to show that the total circuit resistance R is determined mainly by the nonlinear part located in the dynamo-region:

$$R \approx \xi\frac{2I_z^2 l_1 F^2}{c^4 n m_{\rm i}\nu_{\rm ia}\pi r_o^4}\left(1 + \frac{B_z^2(r_o)}{B_\varphi^2(r_o)}\right) \tag{27}$$

This means that the essential steady-state Joule losses for a current-carrying magnetic loop occur mainly in the photosphere.

Slow variations of the current I_z (for the time $t \gg \frac{2\pi}{c}\sqrt{LC}$) in the global electric circuit are described by:

$$\frac{1}{c^2}\frac{\partial(LI_z)}{\partial t} + R(I_z)I_z = \varepsilon \tag{28}$$

where

$$R(I_z) = \frac{l_1}{\pi r_o^2\sigma_1} + \frac{l_2}{\pi r_o^2\sigma_2} + \frac{l_3}{S_3\sigma_3} + \xi_1\frac{l_1 F^2 I_z^2}{c^4 n m_{\rm i}\nu_{\rm ia}\pi r_o^4}\left(1 + \frac{B_z^2(r_o)}{B_\varphi^2(r_o)}\right) \tag{29}$$

$$\xi_1 = \frac{\int_0^{r_o} B_\varphi(1 + \frac{r^2}{r_o^2 b^2})j_z 2\pi r dr}{\pi r_o^2 \bar{B}_\varphi^2(1 + \frac{1}{b^2})\bar{j}_z}$$

The right hand side of Eq. (28) denotes e.m.f. driven by the photospheric convection in the loop footpoints:

$$\varepsilon = \frac{l_1}{c\pi r_o^2}\int_0^{r_o} V_r B_\varphi 2\pi r dr$$

In a self-consistent approach the φ-component of the magnetic field B_φ depends on the current I_z, and hence we can write approximately $\varepsilon = |\bar{V}_r|I_z/c^2 r_o$, where $\bar{V}_r$ is the average value of the radial velocity inside the tube. A typical time scale of

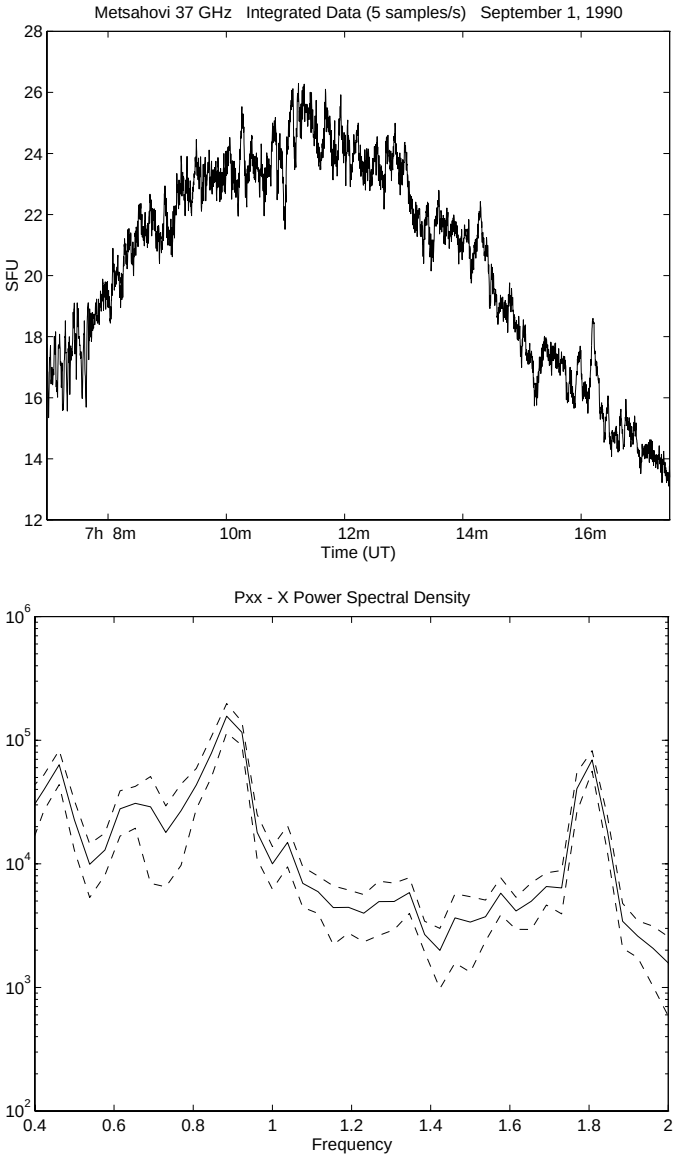

Fig. 3. Part of the Metsähovi burst time profile on September 1, 1990, and its power spectrum

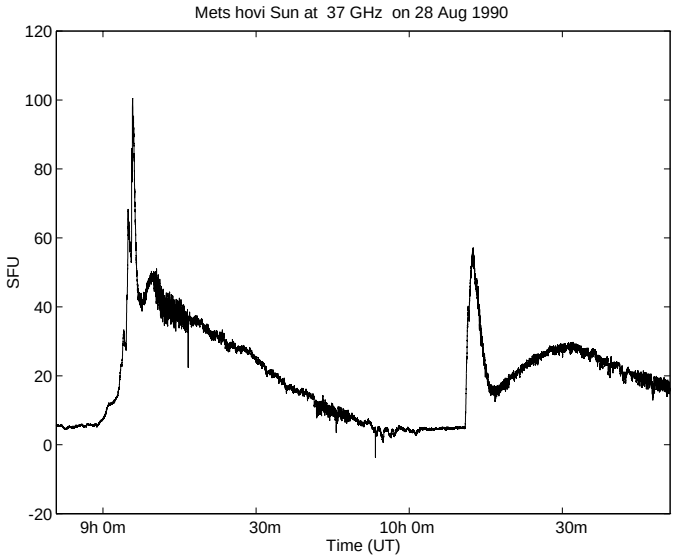

Fig. 4. An example of two homologous bursts with high-Q oscillations, observed at Metsähovi on August 28, 1990

current increase is determined by the minimum value of the two time scales:

$$t_c = min\left\{t_R = \frac{L}{Rc^2};\ t_L = \left(\frac{1}{L}\frac{dL}{dt}\right)^{-1}\right\}$$

Variations of the circuit inductance in time can be dealing with, for example, an emerging magnetic loop. Steady-state current value can be found from the equation $R(I_z)I_z = \varepsilon(I_z)$, and it is easy to show that it coincides with Eq. (10) if the coronal part and the region of current closure in the total circuit resistance are omitted, and the structure coefficient $\xi_1 = 0.5$ when $B_\varphi(r_o) = B_z(r_o)$.

6. Data analysis

To perform the diagnostics of the electrical parameters of the current-carrying magnetic loops we have analyzed flare-associated solar mm-wave bursts observed at the Metsähovi Radio Research Station during 1989-1993. We chose the events with long-term pulsations. The results for sixteen flare bursts measured at 22 GHz (13.5 mm) and 37 GHz (8.2 mm) are given in Table 1. As an example, Figs. 2 and 3 present the temporal behavior of a burst, together with the Pxx - X power spectral density, observed on September 1, 1990. The flare occurred in the NOAA active region 6233 at N13W34, had SN H_α importance, and M2.7 X-ray classification. The fine time-structure of the event reveals the main pulsation period P $\approx$ 1.3 s, which persists throughout the entire burst that lasts for about 30 min. From Table 1 one can see that the pulsation period P varies between 0.7 and 17 s, from event to event, in the bursts under consideration. In the third column of the table radiation fluxes at the burst maximum are given (estimated from spectral slopes if not observed at Metsähovi). Note that as a rule we have analyzed the pulse trains after the burst maximum, e.g., during the period indicated in the second column the mm-wave flux is usually small compared with the burst maximum. The last column in Table 1, with two flare events on 22 June 1989 (Stepanov et al. 1992), and on 7 May 1991 (Urpo et al. 1994), present estimates of the thermal energy of a flare derived from the mm-wave and soft X-ray data.

Changes in the power spectra before, during, and after the bursts were also investigated. The results of the analysis for two homologous bursts on 28 August 1990 are presented in Figs. 4 and 5. One can see that the pulsations have the same period throughout the two events that last for two hours, altogether. This can be considered as an indication in favour of a stable

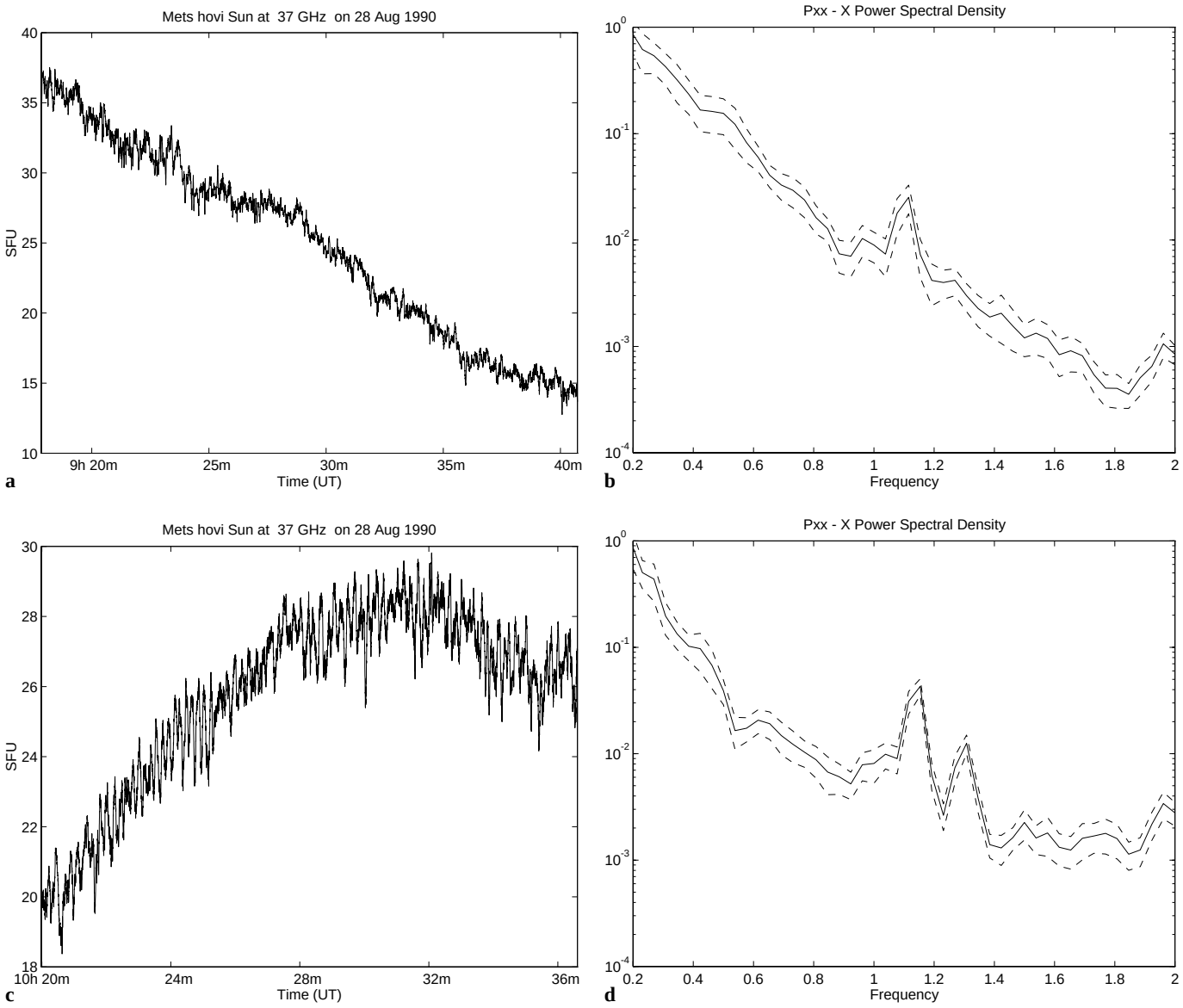

Fig. 5a–d. Parts of the time profiles of the August 28, 1990 bursts, and their power spectra. **a** The burst profile at 09:18-09:41 UT, **b** power spectrum for the burst at 09:18-09:41 UT, **c** the burst profile at 10:20-10:37 UT, **d** power spectrum for the burst at 10:20-10:36 UT

magnetic loop configuration that is not destroyed during the flare.

7. Discussion and conclusions

The current oscillations in a loop result in the modulation of the magnetic field and the loop cross-sectional area. Thus both thermal and nonthermal emission from the loop should be modulated by these oscillations. It follows from Eq. (26) for the capacitance of an equivalent electric circuit, because $l_2/\rho_2 \gg l_1/\rho_1$, that the most important part in the capacitance is the coronal part of a magnetic loop. Supposing, for instance, that $B_\varphi(r_o) = B_z(r_o)$ and $\xi = 0.5$ we get

$$C(I) = \frac{c^4 \rho S^2}{2\pi l I^2} \tag{30}$$

where ρ, l, and S are the average plasma density, length, and cross-sectional area of coronal part of a loop, respectively, and I is the electric current along the loop axis. The total inductance of a slender $(r \ll l)$ flux tube can be presented as (Alfvén & Carlqvist 1967)

$$L = 4\,l\left(\ln\frac{8l}{\sqrt{\pi S}} - \frac{7}{4}\right) \tag{31}$$

From Eqs. (30) and (31) we obtain the period of eigen oscillations of an LRC-circuit

$$P = \frac{2\pi}{c}\sqrt{LC(I)} \approx 10 \times I_{11}^{-1}\ \mathrm{s}\ , \tag{32}$$

where $I_{11} = 10^{-11} I$ A. To find this last Equation we keep in mind the following average values of a magnetic loop (Bray et al.,1991): $n_\mathrm{e} = 10^{10}$ cm^{-3}, $l = 5\times10^9$ cm, and $S = 10^{17}$ cm^2.

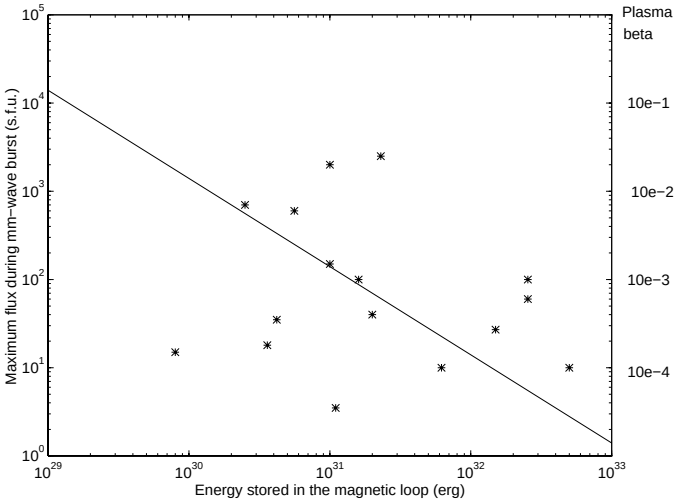

Fig. 6. Maximum fluxes of the observed mm-wave bursts (stars), and the plasma β (solid line), vs. the energy stored in a coronal loop

The current values inferred from Eq. (32) are given in Table 1 for the events under investigation. For these sixteen events the values of the total circuit energy $LI^2/2c^2$ are also presented. These values are between 3.6×10^{30} and 5×10^{32} ergs. For two of the events, 22 June 1989 and 7 May 1991, we got a chance to compare the total energy stored in the circuit and the thermal energy of the flare. For the 22 June 1989 flare we obtained the current $I = 2 \times 10^{11}$ A and $LI^2/2c^2 = 10^{31}$ ergs. On the other hand the thermal energy of the evaporated plasma, inferred from mm-wave and soft X-ray data (Urpo et al. 1994), is equal to $E_{\rm th} = (1.0 - 4.5) \times 10^{29}$ ergs. For the flare of 7 May 1991, we got $LI^2/2c^2 = 3.6 \times 10^{30}$ ergs and the thermal energy of the flare was $E_{\rm th} = (1.2 - 1.8) \times 10^{29}$ ergs. The thermal energy of a hot evaporated chromospheric plasma filling the magnetic loop is about the total flare energy (Wu et al. 1986). Hence, at least for these two flares we can claim that only 5% of total energy of the electric current stored in the current-carrying magnetic loop was released during a single flare process. Such a situation seems quite reliable when the magnetic structure is stable trough the entire flare. One example of homologous flares having almost the same time behavior, demonstrated by the similarity in Pxx-X power spectral densities, is shown in Fig. 5. A rather good example has also been presented before by Urpo (1983). Fig. 6 shows the dependence of the maximum flux of a mm-wave burst vs. the total energy stored in the circuit, see also Table 1. The tendency is to have a decreasing mm-wave plasma flux with the increase of the total circuit energy. We interpret this tendency in terms of plasma beta $\beta = 8\pi nkT/B^2 \approx 2 \times 10^{28} (LI^2/2c^2)^{-1}$. The plasma beta decreases when the stored energy increases, because the magnetic field in the loop grows. In the case of a low beta plasma the plasma instabilities, for example the flute-instability which can act as a flare trigger (Zaitsev & Stepanov 1992), are stabilized ('hard' circuit) and the energy release drops.

Note, that the Q-factor $Q = \frac{1}{cR}\sqrt{C/L}$ of current oscillations is high enough. Indeed, taking Eqs. (30) and (31) into account for $R = R_1 = 10^{-6}\,\Omega \approx 10^{-18}$ CGS we get $Q \approx 10^6$. Under flare condition $R = 10^{-3} - -10^{-4}\,\Omega$ and $Q \approx 10^3 - -10^4$.

The self-consistent model of an equivalent circuit analog for the current-carrying magnetic loop that has been considered here, suggests relatively powerful long-duration Joule energy release in the loop footpoints in the photosphere. For the case of a steady-state flux tube, the kinetic energy of a solar plasma convective flow in the footpoints gives DC electric field that is due to the charge separation (Sen & White 1972). The power connected with the plasma flow is realized in the form of Joule heating

$$q = \left(\mathbf{E} + \frac{1}{c}\mathbf{V} \times \mathbf{B}\right)\mathbf{j}\,.$$

For the axially symmetric magnetic flux tube with $\mathbf{B}(0, B_\varphi(r), B_z(r)), \mathbf{j}(0, j_\varphi(r), j_z(r))$ and partially ionized plasma flow $\mathbf{V}(V_r, 0, V_z)$, keeping in mind Eq. (5), we obtain for $\alpha\mathbf{B}^2 \gg 1$ that the Joule energy dissipation is independent of the magnetic field: $q = nm_{\rm i}\nu_{\rm ia}v_r^2(r)/F$. Our estimates have shown that for the convection velocities 0.3–0.5 km/s that are usually observed (Bray et al. 1984; Simon & Leighton 1964), the Joule heating input is less as compared with the radiation losses, and the loop footpoints remain cool ($\approx 4 \times 10^3$ K). If the velocity of the convective flow grows up to extreme values, ≈ 2 km/s, the Joule heating becomes more important than the radiation losses and the loop legs can be heated a lot. Such a heating may be one origin for the observed soft X-ray bright points (Bray et al.,1991).

Let us summarize the main results in our analysis. A self-consistent model of an equivalent LRC-circuit analog of the current-carrying magnetic loop reveals that both the resistance and the capacitance depend on the electric current along the loop axis. Quasi-periodic modulation of the mm-wave emission during a flare is the radiation signature of the eigen oscillations of an LRC-circuit and include the information on the current value in a magnetic loop. Spectral analysis of the sixteen mm-wave events presented in this paper give modulation time scales from 0.7 to 17 s, which, in turn, give current values $I \approx 6 \times 10^{10} - 1.4 \times 10^{12}$ A and total circuit energies $LI^2/2c^2 \approx 10^{30} - 5 \times 10^{32}$ ergs. We got the possibility to compare the total energy of the current stored in a loop and the flare energy for two of the events. In both cases the flare energy was less then 5% of the total circuit energy. It means that the magnetic structure of the flare loop or the loop system was stable and didn't change during the flares. There was a tendency of decrease in the maximal mm-wave emission flux (and most probably the total flare energy) with the increase of the energy stored in the magnetic loop in the sixteen flares that were investigated.

In conclusion we point out that the method of electric current diagnostics proposed here can be applied to the diagnostics of currents in stellar atmosphere. The loop size in the coronae of UV Cet-type stars is about an order of magnitude bigger as compared to the solar case. Taking for example the pulsation period observed on Hyades flare star H II 2411 by Rodono (1974), equal to 13 s, and using Eqs. (30) and (32) for the pulse period

we have $I \approx 3 \times 10^{12}$ A and, consequently, the total energy stored in a stellar magnetic loop is $LI^2/2c^2 \approx 3 \times 10^{35}$ ergs.

Acknowledgements. The authors wish to thank Juho Heikkilä for technical assistance with the manuscript. This work was supported by INTAS-RFBF grant 95-0316, and RFBF grants 96-02-16045a and 96-02-16972, and by the Academy of Finland.

References

Alfvén H., & Carlqvist P., 1967, Solar Phys. 1, 220
Andrews A.D., 1990, A&A, 229, 504
Anzer U., 1978, Solar Phys. 57, 111
Bray R.J., Loughhead R.E., & Durrant C.J., 1984, The Solar Granulation, Cambridge Univ. Press
Bray R.J., Cram L.E., Durrant C.J., & Loughhead R.E., 1991, Plasma Loops in the Solar Corona, Cambridge Univ. Press
Conti P.S. & Underhill A.B., 1988, O Stars and Wolf-Rayet Stars, NASA SP-497
Doyle J.G., van den Oord G.H.J., Butler C.J., & Kiang T., 1990, in L.V. Mirzoyan et al. (eds.), Flare Stars in Star Clusters, p. 325
Hagyard M.J., 1989, Solar Phys. 115, 107
Hénoux J.C. & Somov B.V., 1987, A&A, 185, 306
Houdebine E.R., Foing B.H., Doyle J.G., & Rodono M., 1993, A&A, 274, 245
Hudson H.S., 1987, Solar Phys. 113, 315
Ionson J., 1982, ApJ, 254, 318
Kan J.R., Akasofu S.-I., & Lee L.C., 1983, Solar Phys. 84, 153
Kaufmann P., Piazza L.R., & Rafaelli J.C., 1977, Solar Phys. 54, 179
Klimchuk J.A., Lemen J.R., Feldman U., et al., 1992, PASJ, 44, L181
Kuperus M. & Raadu M.A., 1974, A&A, 31, 189
Leka K.D., Canfield R.C., McClymont A.N., et al., 1993, ApJ, 411, 370
Martens P.C.H., 1987, Solar Phys. 107, 95
Melrose D.B., 1991, ApJ, 381, 306
Melrose D.B., 1995, ApJ, 451, 391
Melrose D.B. & McClymont A.N., 1987, Solar Phys., 113, 241
Miller M.C., Lamb F.K., & Hamilton R.J., 1994, ApJS, 90, 833
Mullan D.J., Herr R.B., & Bhattacharya S., 1992, ApJ, 391, 265
Rodono M., 1974, A&A, 32, 337
Sen H.K. & White M.L., 1972, Solar Phys., 23, 146
Severny A.B., 1965, Space Sci. Rev., 3, 451
Simon G.W. & Leighton R.B., 1964, ApJ, 140, 1120
Spicer D.S., 1982, Space Sci. Rev., 31, 351
Stepanov A.V., Urpo S., & Zaitsev V.V., 1992, Solar Phys., 140, 139
Thomas R., Neupert W., & Thompson W.T., 1987, in Rapid Fluctuations in Solar Flares, NASA Conf. Publ. 2449, p. 299
Urpo S., 1983, Adv. Space Res. 2, No 11, 105
Urpo S., Bakhareva N.M., Zaitsev V.V., & Stepanov A.V., 1994, Solar Phys., 154, 317
Van Tend W. & Kuperus M., 1978, Solar Phys., 59, 115
Wu S.T., de Jager C., Dennis B.R., et al., 1986, in M. Kundu & B. Woodgate (eds.), Energetic Phenomena on the Sun, NASA Conf. Publ. 2439, p. 5-1.
Wülser J.-P. & Kämpfer N., 1987, in Rapid Fluctuations in Solar Flares, NASA Conf. Publ. 2449, p. 301
Zaitsev V.V., 1996, in Y. Uchida et al. (eds.), Magnetodynamic Phenomena in the Solar Atmosphere - Prototypes of Stellar Magnetic Activity, Kluwer, p. 317
Zaitsev V.V., 1997, in H.K. Biernat et al. (eds.), The Solar Wind-Magnetosphere System 2, Proc. Int. Workshop, Graz, 1995, p. 61
Zaitsev V.V., & Khodachenko M.L., 1997, Radiophys. Quantum Electronics, 40, 114
Zaitsev V.V. & Stepanov A.V., 1982, SvAL, 8, 132
Zaitsev V.V. & Stepanov A.V., 1988, SvAL, 14, 456
Zaitsev V.V. & Stepanov A.V., 1989, SvAL, 15, 154
Zaitsev V.V. & Stepanov A.V., 1992, Solar Phys., 139, 343
Zarro D.M., Saba J.L.K., & Strong K.T., 1987, in Rapid Fluctuations in Solar Flares, NASA Conf. Publ. 2449, p. 289
Zlobec P., Messerotti M., Dulk G.A., & Kucera T., 1992, Solar Phys. 141, 165